Chemosphere, Vol.27, No.11, pp 2127-2142, 1993
Printed in Great Britain

0045-6535/93 $6.00 + 0.00
Pergamon Press Ltd.

PHOTOOXIDATION OF EXHAUST POLLUTANTS

I. Degradation efficiencies, quantum yields and products of benzene photooxidation

Kamps,R.[a]; Müller,H.[b]; Schmitt,M.[b]; Sommer,S.[a]; Wang,Z.[a]; Kleinermanns,K.[a*]

a) Institut für Physikalische Chemie und Elektrochemie I, Heinrich-Heine-Universität Düsseldorf;
b) Physikalisch-Chemisches Institut, Universität Heidelberg;
*) to whom correspondence should be adressed

(Received in Germany 24 May 1993; accepted 27 July 1993)

Abstract

The photochemical decomposition and oxidation of benzene was investigated in the gas phase by irradiation of benzene in an oxygen/ozone atmosphere with ultraviolet light from low and medium pressure mercury lamps. The degradation efficiency depends on the concentration of the pollutant, the power output of the UV-lamp, the ozone concentration and the residence time in the irradiated area.
The quantum yields for photooxidation at 1 atm O_2 without addition of O_3 were measured to be $<< 1$, both at 185 and 254 nm, demonstrating loss channels of the electronically excited benzene which are fluorescence, internal conversion and intersystem crossing as well as the absence of chain reaction steps at both wavelengths.

1. Introduction

Organic solvents play a vital role in a variety of industrial processes, e.g. in paint applications, in adhesives, for degreasing and cleaning metals, in dry cleaning or in the chemical industry generally. Here, especially chlorine-containing solvents represent a hazard for the environment because of their inefficient biological degradation, their relative high toxicity and their long lifetimes. Their role in the atmospheric decomposition of ozone has been discussed frequently.
The preparation and processing of these solvents leads to the problem of contamination of soil or air by highly organically contaminated exhaust air. In recent years the requirements for purification of exhaust gases have

become more stringent. Conventional procedures to decontaminate exhaust gases from organic compounds are absorption, combustion, condensation, biological filtration, chemisorption and oxidation by ionising radiation. Recent methods to decontaminate gaseous pollutants are based on their adsorption on activated charcoal. The gaseous pollutants are directed over activated charcoal, which has to be deposited in highly protected refuse dumps after use if regeneration is not possible or if the solvent required to regenerate the coal has to be combusted in special incinerators. This technique is sometimes no more than a displacement of the problem.
For highly volatile compounds like monochloroethene this procedure is of not applicable, because of their incomplete adsorption on activated charcoal.
Thermal or catalytic combustion as an alternative method is expensive and, in the case of small emission rates, as found in dry cleaning, printing works and other intermediate enterprises using organic solvents, also unpractical. The decontamination of exhaust pollutants based on extraction from soil by pumping is hardly practical in infrastructurally less open areas, like refuse dumps or old industrial plants. Combustion is only possible using a flue gas washer. Additionally, the corrosive nature of the flue gases damage equipment and poison the catalyst, if used.

Photooxidation of waste air is a physicochemical process to destroy organic pollutants. The oxidation of the pollutants is initiated by UV-radiation at room temperature and normal pressure. The mechanism of the oxidation is a radical chain reaction in many cases. The gas stream is irradiated by UV-lamps with suitable power and spectral distribution.
The reaction parameters have to be optimized, because the final goal is to obtain nontoxic or easy to handle products like HCl, carbon dioxide and water. Acid products like HCl can be removed by conventional wet cleaning.
The most important solvents in contaminated soils are monochloromethane, dichloromethane, trichloromethane, tetrachloromethane, 1,1,1-trichloroethane, monochloroethene, dichloroethene (especially cis-1,2-dichloroethene), trichloroethene and tetrachloroethene. Besides, in many cases the soil is contaminated by aromatic solvents like benzene, toluene, xylenes and sometimes ethylbenzene.
Paper I of this series deals with the photooxidation of benzene, while paper II and III concentrate on the UV-oxidation of chloromethanes and chloroethenes respectively.

2. Experimental

Fig. 1 shows the experimental set-up for our investigations of photooxidation in the gas phase. Air was bubbled through the hydrocarbon liquid and allowed to flow into the glas irradiation chamber via an adjustable ring jet. The hydrocarbon concentration depends on its vapour pressure and can be adjusted by temperature variation in a cold bath. The oxygen/ozone mixture flowed from the bottom into the reactor. By using this arrangement it is

possible to adjust irradiaton and reaction time by changing the height of the ring jet along the irradiation zone. GC-ECD, GC-MS and FTIR analysis were used for identification of the reaction products.

A bar-shaped, medium pressure mercury lamp (Heraeus TQ 150, power 150 W) is centered in the reactor. The ozone concentration in the O_2/O_3 mixture was adjusted by the voltage of the ozoniser (Argentox GL) and calibrated by the "Hartley-band" absorption of O_3.

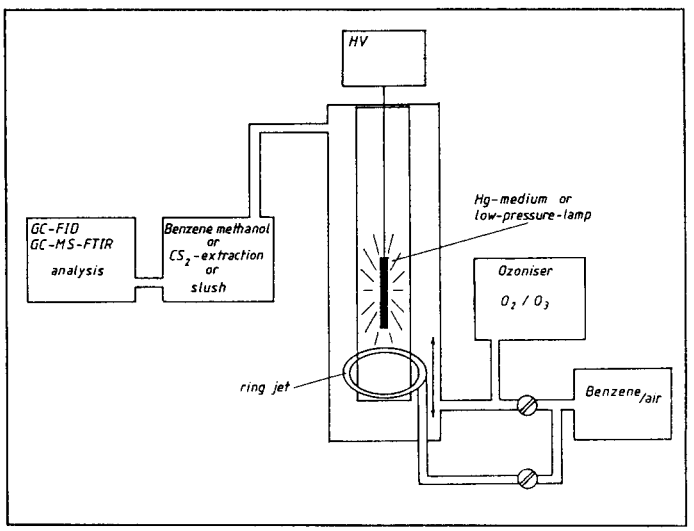

Fig.1 Experimental set-up for photooxidation of (halogenated and aromatic) hydrocarbons in the gas phase

The reactor works as a free flow system. Therefore it is possible to calculate concentrations via the flow velocity of the compounds, the partial pressure in the mixture and the atmospheric pressure:

$$\frac{v_1}{v_2} = \frac{p_1}{p_2} \qquad (1)$$
$$p_1 + p_2 = p$$

Here v_1 and v_2 are the O_2/O_3- and hydrocarbon/air flow velocities respectively, p_1 and p_2 are their partial pressures and p is the atmospheric pressure.

The flow velocity of the O_2/O_3 mixture is chosen to be higher than the hydrocarbon/air mixture to prevent a hydrocarbon back flow below the ring jet. In this manner a defined variation of the hydrocarbon residence time in the irradiation zone is possible by adjusting the height of the ring jet. Behind the reactor the gas mixture flows either through activated charcoal as adsorbent, which is then extracted by CS_2, or through benzene methanol as

solvent. The solution is analysed by direct injection gas chromatography (Carlo Erba Instruments Fractorap 4100; HP-Integrator 3390 A; Chrompack WCOT quartz capillary tube with 52 m length, ID 0.32 mm, 1.3 μm CPsil 8CB; FID or Perkin Elmer Sigma 2000; Perkin Elmer quartz capillary tube, Permaphase PVMS/54 with 50 m length, I.D. 0.32 mm; FID). Total irradiation time was typically 5 minutes.

For sensitive analysis of side products, irradiation times of 3-8 hours were chosen with product accumulation in the cold trap of an acetone/N_2-slush at -70°C. Qualitative analysis, i.e. identification was performed by GC-MS analysis combined with computer-aided mass spectrometry library search. The instruments used were a GC Varian 1700; CH7A Finnigan MAT; INCOS Data System Finnigan Mat and a Hewlett Packard GC/FTIR-MS with GC 5890 Series II; MS 5971 with the Wiley library and FTIR 5965B with the EPA REVA library. Qualitative analysis of fragile side products which cannot pass the GC capillary tube without decomposing was performed by FTIR analysis (Hewlett Packard FTIR Series 1600). For these measurements, a 15 W low pressure mercury lamp was positioned in front of the reaction vessel in the optical path of the sample area of the FTIR-spectrometer. In this arrangement we performed measurements under stationary conditions with residence times up to 15 minutes. Quantitative side product analysis was performed by gas chromatography.

To ensure monochromatic irradiation we used a chamber provided with two different UV-filters. The filters (either ozone or $NiSo_4/CoSO_4$) were placed between the rod-shaped, low pressure Hg-lamp and the irradiation chamber. Two different lamps were used with 20 or 15 W respectively.

To eliminate 254 nm radiation when using the 20 W Hg-lamp, ozone (ozone generator Argentox GLX 3) flowed constantly through the cell as a filter (optical path length: 1cm). Indeed, we could demonstrate (UV-spectrometer Perkin Elmer 555) that 99.3% of the emitted light at 254 nm was absorbed (Hartley-Band). Using ozone as a filter automatically leads to a decrease of lamp intensity at 185 nm ($\approx$20%) because of the absorption of residual O_2 at this wavelength ($\sigma_{oxygen,185\,nm} = 9.3*10^{-21}$ cm^2 [1]).

On the other hand, measurements at 254 nm were realized using the 15 W lamp and the $NiSO_4/CoSO_4$-filter to eliminate 185 nm radiation. This liquid filter is easily made by dissolving 500 g $NiSO_4 \cdot 6H_2O$ and 75 g $CoSO_4 \cdot 7H_2O$ in 1000 ml H_2O [32]. A check on the absorption capacity by UV-measurement showed that 99.4% of the 185 nm radiation was eliminated.

Measurement of pressure:

- benzene / acetone by using the vapour pressure at different temperatures
- ozone by UV-spectroscopy
- ethene by using gas chromatography

The substances used:

- benzene, p.a. (Fluka) 99,5%
- acetone, p.a. (Riedel deHaen) 99,5%
- ethene 3.5 (Messer Griesheim)
- oxygen 4.8 (Messer Griesheim)

- nitrogen 5.0 (Messer Griesheim)
- ozone, ozone generator Argentox type GLX 3
- $NiSO_4 \cdot 6H_2O$, (Aldrich) 99%
- $CoSO_4 \cdot 7H_2O$, (Aldrich) 99%

3. Results

3.1 Dependence of degradation efficiency on hydrocarbon concentration

Fig. 2 shows the dependence of benzene degradation on the benzene partial pressure. The O_2/O_3 flow in this experiment was 500 ml/min with an ozone concentration of 150 ppm.

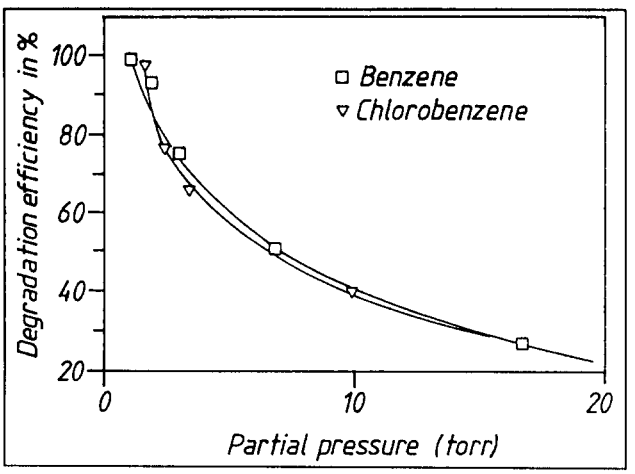

Fig.2 Degradation efficiency as a function of the benzene concentration. $[O_3] = 3.1 \cdot 10^6$ mol/l (150 ppm), 150 W medium pressure Hg-lamp, 7s residence time

The benzene partial pressure was changed by varying the benzene/air flow according to equation (1). The power output of the UV-lamp was 150 W. The residence time of benzene in the irradiation zone can be calculated to be 7 seconds at the total flow of the experiment. Increasing of the benzene concentration obviously reduces the degradation efficiency. This reduction depends on the lamp power, i.e. at higher lamp power the degradation curve shifts to higher benzene partial pressures.

3.2 Dependence of degradation efficiency on residence time

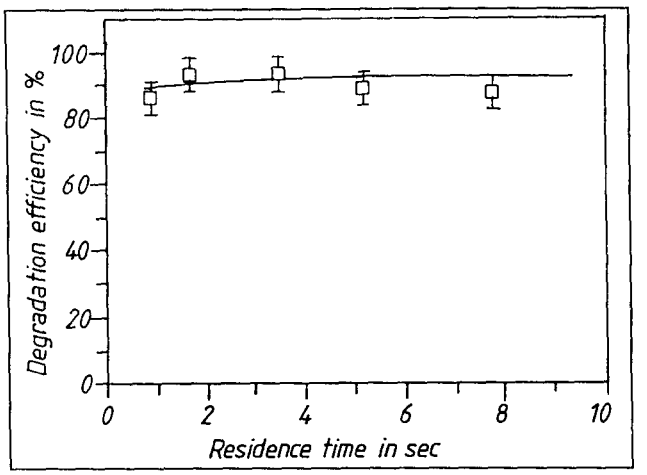

Fig.3 Degradation efficiency of benzene in dependence of the residence time in the irradiated volume. $[O_3] = 3{,}1 \cdot 10^6$ mol/l (150 ppm), 150W medium pressure Hg-lamp, 2.2 torr benzene

By varying merely the ring jet position only the residence time is changed while all other conditions (benzene-, ozone concentration, lamp power) stay constant. Nearly complete decomposition of 2.2 torr benzene can be achieved at residence times of $\geq$ 1 sec, cf. Fig. 3.
At times > 1 sec the degradation of benzene is nearly independent of the residence time. Obviously benzene photooxidation occurs on a quite fast time scale, even at the low lamp power used here.

3.3 Dependence of degradation efficiency on ozone concentration

Variation of ozone concentration at constant benzene partial pressure (1.2 torr) shows that even small concentrations of $\leq$ 150 ppm ozone are sufficient to decompose benzene efficiently. Above a certain threshold concentration the degradation efficiency becomes independent of ozone concentration.

Obviously, ozone photodissociation starts a fast and efficient radical process which decomposes benzene. The photodissociation and oxidation of benzene is not very effective, as shown in section 3.5. Therefore it is advantageous to use a radical starter, such as oxygen atoms from O_3 photodissociation [1,2].
We cannot exclude that sufficient ozone is formed "in situ" by the 150 W Hg-lamp irradiation of O_2 to accelerate benzene decomposition, so that the 40 % degradation efficiency in fig. 4 with "no ozone" added is indeed an upper limit.

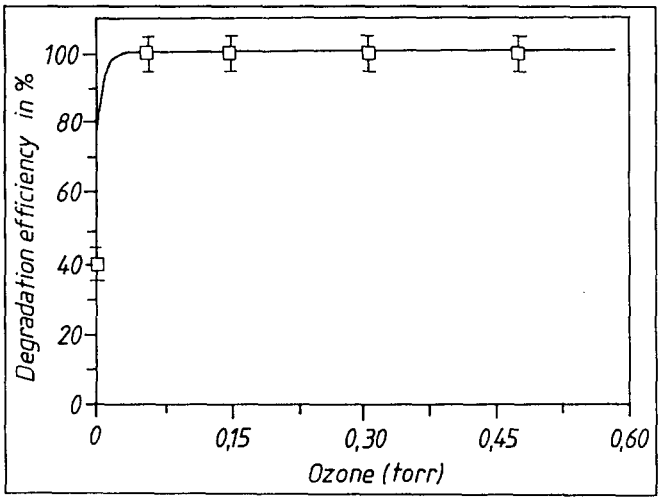

Fig.4 Degradation efficiency of benzene as a function of ozone partial pressure. 1.2 torr benzene, 150W medium pressure Hg-lamp, 7s residence time

3.4 Degradation products

Qualitative determination of main and side products were realized by GC-MS-analysis (MS Varian Type CH7A, GC Varian Type Aerograph Series 1700; fused silica capillary tube OV1, 25 m length).
Phenol, biphenyl, benzoic aldehyde, maleic acid anhydride, p-benzochinone and toluene were identified as main side products [fig. 5].

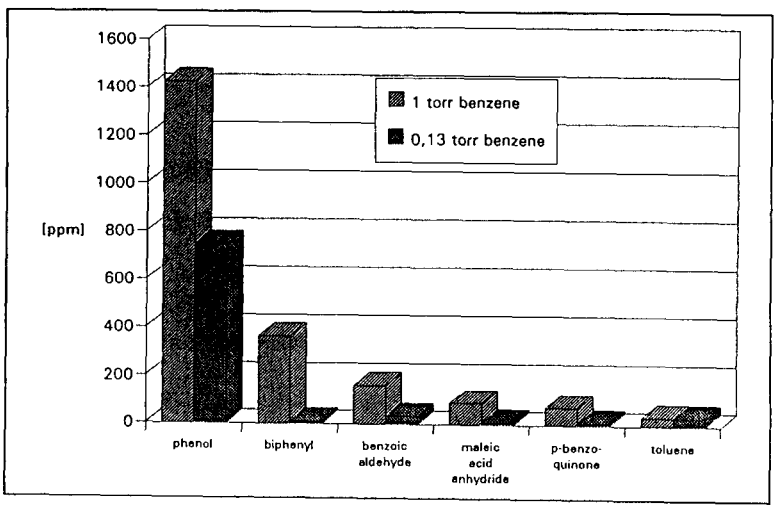

Fig.5 Main products of benzene degradation at 1 torr and 0,13 torr benzene partial pressure using a 350W high pressure mercury lamp.

Ethoxybenzene, dihydroxybenzene, hydrochinone, cyclohexanone, benzoic acid and cresol isomers were found at concentrations below 10 ppm.

Small amounts of formic acid were identified by FTIR-spectroscopy (Perkin Elmer FTIR-Spectrometer, Series 1600) at long irradiation times of 15 minutes. Here the low pressure Hg-lamp was mounted outside of the FTIR-cell and the corresponding low lamp intensity necessitated long irradiation times.

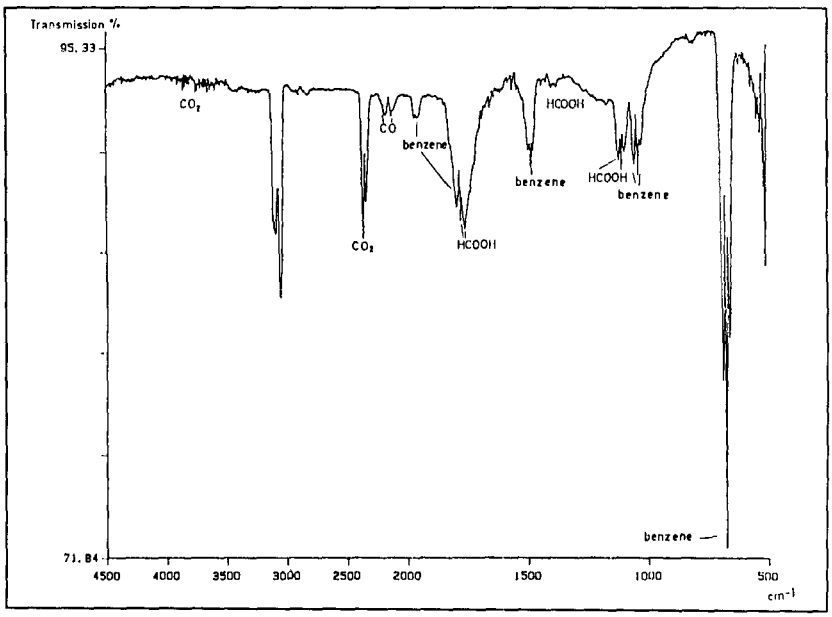

Fig.6 FTIR-spectrum of 5 torr benzene after irradiation for 15 minutes in an oxygen atmosphere using a 15W low pressure mercury lamp.

3.5 Quantum yields of benzene photooxidation

The quantum yield of a photochemical process can be obtained by measuring the absolute intensity of the incident light and the fraction of light absorbed by the reactant in the reaction vessel of a certain length as well as the number of degraded molecules.

In "chemical actinometry" a secondary standard is used for which the quantum yield has been well established. As chemical actinometer for the ultraviolet region, acetone and ethene photolysis were used for 254 and 185 nm irradiation respectively.

The degradation efficiency of the standards and benzene were measured at different concentrations under photooxidation and photolysis conditions respectively with the same lamp power and flow reactor geometry.

The quantum yield is defined as follows:

$$\phi_x = \frac{number\ of\ degraded\ molecules\ x}{number\ of\ absorbed\ photons} \qquad (2)$$

or using the Lambert-Beer-Law:

$$\phi_{x,t} = \frac{\Delta[x]_t}{I_o \cdot (1 - e^{-k_x \cdot [x]_t \cdot l})} \qquad (3)$$

here $\Delta[x]_t$ is the concentration change of x after a certain time t by photooxidation and I_o the incident light intensity passing through a flow reactor of effective absorption path length l containing the gas x with an absorption coefficient k_x at a certain concentration $[x]_t$. We measured at small Δx values, so that $[x]_t \cong [x]_{t=0}$.
With a similar expression for photolysis of the standards, e.g. acetone one obtains:

$$\phi_x = \frac{\Delta\ [x]_t \cdot (1 - e^{-k_{Ac} \cdot [Ac]_t \cdot l})}{\Delta\ [Ac]_t \cdot (1 - e^{-k_x \cdot [x]_t \cdot l})} \cdot \phi_{Ac} \qquad (4)$$

The quantum yield of benzene photooxidation at concentrations of 6, 1 and 0.1 torr benzene was determined to be $\phi_x \simeq 0.05 \pm 0.02$ at 254 nm using an $NiSO_4$-filter to eliminate $\approx$ 99 % of the 185 nm radiation from the low pressure Hg-lamp.
When using an O_3-filter to eliminate > 99 % of the 254 nm radiation and ethene photolysis as actinometer reaction, a quantum yield ϕ_x(185 nm) $\simeq 0.01 \pm 0.005$ was determined at 1 and 0,1 torr benzene respectively. The filter absorptivities were checked by UV-absorption.
Error sources are mainly the uncertainties of the absorption coefficients of benzene, acetone and ethene as well as the reference actinometer quantum yields.
For acetone decomposition the quantum yield is between 0.5 and 1.0 depending on cell temperature as discussed in refs. [18,19,20]. For ethene decomposition the quantum yield for C_2H_4-disappearance is known to be $\approx$ 1 [17] resulting from:

$$C_2H_4 + h\nu(\lambda=185nm) \rightarrow C_2H_2 + H_2 \ ; \ \phi = 0.68$$
$$C_2H_2 + 2H \ ; \ \phi = 0.20$$
$$C_2H_3 + H \ ; \ \phi = 0.16$$

Indeed, we took the quantum yield of ethene to 0.7 because of its dependence on the inert gas pressure [17]

which leads to a reduction of about 30% comparing 0 torr and 760 torr N_2-pressure.

In any case, the quantum yield for benzene photooxidation both at 254 and 185 nm is considerabely below one, demonstrating the absence of chain reactions and importance of loss mechanisms, which are fluorescence, internal conversion and intersystem crossing, c.f. ref [3]. This can be compared with the pure photolysis of benzene. Here no significant chemical change was observed in the gas phase at 254 nm while quantum yields of near unity were found for benzene disappearance at 185 nm at the low pressure limit which decreases with increasing gas pressure [22].

For determination of absorption cross sections we decided to use a narrow band Hg-low pressure lamp (Osram HNS 20/U) with defined emission bands at 185 nm and 254 nm. The majority of the absorption cross sections given in literature are taken from absorption spectra of benzene from broadband spectrometers. Benzene as well as acetone, however, show structured absorption spectra in the 254 nm region so that the absorption cross sections depend fundamentally on the spectrometer bandwidth. We therefore measured the absorption cross section with the Hg-lamp directly and found them to be considerably higher (table I) than the broadband values in the literature (aceton: $\sigma_{254nm} = 3.1*10^{-20}$ cm^2 [20], benzene: $\sigma_{254nm} = 3.8*10^{-19}$ cm^2 [3] with hexane as solvent). We carefully excluded mercury in the system.

The comparison however shows that both absorption coefficients rise by a factor of roughly five so that the quantum yields obtained with both sets of cross sections do not differ much.

Table I. Absorption coefficients and quantum yields of benzene photooxidation at 185 and 254 nm. The 15W low pressure mercury lamp is equipped with an O_3- and $NiSO_4$-filter respectively.

	Benzene	**Acetone**	**Ethene**
Absorption cross section σ [cm^2]			
at 254 nm	$1.8*10^{-18}$	$1.8*10^{-19}$	-
at 185 nm	$2.5*10^{-17}$	-	$3.1*10^{-19}$
Quantum yields ϕ			
at 185 nm	0.01	-	0.7
at 254 nm	0.05	0.5	-

A second method for determination of quantum yields is the use of a laser where it is easy to establish the number of absorbed photons directly. Using an irradiation chamber with defined volume and benzene concentration one can measure the laser intensity before and after passing the reaction vessel, after correction for window transmission, to obtain direct information on the number of absorbed photons.

The initial benzene concentration as well as the concentration after photooxidation by 266 nm laser light from a quadrupled Nd-YAG-Laser (HY 750, Lumonics) is obtained by quantitative FTIR-spectroscopy. A low pulse

energy flux of 72 $\mu J/cm^2$ was chosen to minimize multiphoton effects.
The number of absorbed photons per second is calculated from the number of photons in a single laser pulse, the pulse repetition rate and the benzene absorption coefficient at 266 nm.
Again we obtain quantum yields below one, demonstrating the absence of chain reaction steps for benzene photooxidation in its first absorption band. ϕ_x is somewhat higher here than in the lamp experiment, but laser excitation may lead to special loss processes like multiphoton dissociation and ionisation despite the low laser energy flux chosen here.

As shown in Fig. 4, ozone addition leads to a significant increase in benzene degradation efficiency. We therefore decided to measure the quantum yield of ozone-sensitized photooxidation also. The quantum yield is defined here by the number of absorbed photons from benzene and ozone absorption. We again obtained quite low quantum yields: $\phi_x(O_3\text{-sens.}; 254\ nm) = 0{,}05 \pm 0{,}02$.
Both, the degradation efficiency after O_3 addition and the number of absorbed photons are substantially higher. Altogether, the quantum yield does not change much. This points to the absence of chain reaction steps for ozone-sensitized benzene photooxidation. Ozone addition merely opens another non-chain branching channel for attack on benzene and this is described in the next section.

4. Discussion

The measured photooxidation quantum yields can be compared with the photolysis quantum yields at low pressure or in an inert gas atmosphere. Regarding benzene photolysis at 184.9 nm [4,21,22], the quantum yield for disappearance of benzene was found to be unity at low pressure but to decrease substantially below one with increasing benzene or N_2 buffer gas pressures. The main photoproducts were identified as fulvene, an isomer of benzene [4,23,24] and polymers as cis- and trans-1,3-hexadien-5-yne [4,25,26] as well as small amounts of methane, ethane, ethylene, hydrogen and acetylene [4,21,27]. Lee et al. [4] showed that laser photolysis of benzene at 193 nm occurs under collisionless conditions through three primary channels, namely, $C_6H_6 + H$ (80%), $C_6H_4 + H_2$ (16%) and $C_5H_3 + CH_3$ (4%).
From the pressure dependence of the quantum yield for benzene disappearance it is proposed that internal conversion (IC) from the electronically excited singlet state ($^1E_{1u}$ or $^1B_{1u}$) populated by 184.9 nm absorption leads to "hot benzene", i.e. vibrationally highly excited, electronic ground state benzene molecules (S_0^*) which subsequently isomerize to give various hot benzene isomers, probably fulvene. The vibrationally hot isomers collisionally stabilize or react to form dissociation products and polymers.
The lifetime of the S_2-state is reported to be 20 ps [4,29] and most of the molecules in S_2 relax to S_0^*. At atmospheric pressure, most of the S_0^*-benzene molecules are collisionally quenched to vibrationally comparatively cold S_0-benzene which does not react further. This explains the decrease in quantum yield for benzene disappearance at 185 nm with increasing pressure.

The low quantum yields for benzene photooxidation at 185 nm measured here show that exchange of N_2 by O_2 does not change this overall picture very much. Most of the excited benzene molecules are merely quenched to electronic ground state benzene without reaction. The small benzene degradation observed here is probably partly from O_3 and O-atom attack on benzene from spurious amounts of ozone formed by 185 nm photolysis of oxygen at atmospheric O_2-pressure.

When gaseous benzene is excited at 254 nm to the lowest excited singlet S_1- ($^1B_{2u}$-) state, it is known to relax through IC [4,11], intersystem crossing [4,30] to the triplet state, fluorescence [4,30] and isomerisation to benzvalene [4,30,31] without any evidence of dissociation. The quantum yield for benzene disappearance at 254 nm in an inert gas atmosphere is known to be close to zero [3]. Lee et al. [4] showed that new photodissociation channels open up at 248 nm photolysis under collision-free conditions, because the hot benzene molecules are no collisionally relaxed and can dissociate. Two primary dissociation channels, $C_6H_4 + H_2$ (96%) and $C_5H_3 + CH_3$ (4%) were observed [4]. At atmospheric pressure, however, these channels are quenched.
Again, 254 nm photolysis in an O_2 atmosphere does not change things substantially. Mainly S_1-benzene is quenched so that little reaction takes place, leading to quantum yields $<<$ 1. The higher 254 nm quantum yield [Table I] is possibly due to some minor reactive quenching of electronically excited benzene with O_2. Ozone- and O-attack on benzene does not play a role at 254 nm with an "ozone-free" Hg-lamp and a $NiSO_4$-filter.

The rather efficient benzene degradation with the 150 W medium pressure Hg-lamp and the 300 W high pressure Hg-lamp (fig. 1-4) is therefore, in our opinion, mainly due to photolysis of the added ozone and attack of O-atoms on benzene. Even if no ozone is added (c.f. fig. 4) the intense Hg-lamps used here may produce sufficient ozone from air photolysis to enhance benzene degradation by O-atom attack. Thermal heating by these intense lamps will accelerate benzene degradation to some extent also. In the following we describe a mechanism for O-attack on benzene and subsequent reactions which we regard as the most important pathway in benzene photooxidation.

The photodissociation of ozone in the "Hartley band" (200 nm - 300 nm) creates ^1D-oxygen atoms, which are quenched by molecular oxygen or nitrogen to ^3P-oxygen [1,2]:

$$O_3 + h\nu \Rightarrow O(^1D) + O_2(^1\Delta)$$

$$O(^1D) + O_2(N_2) \Rightarrow O(^3P) + O_2(N_2)$$

^3P-oxygen adds to benzene under formation of a triplet-diradical intermediate (C_6H_6O), which can react according to [5,6,7,8] by

a) abstraction of a hydrogen atom and formation of a phenoxy

radical (C_6H_5O);

$$C_6H_6 + O(^3P) \Rightarrow (C_6H_6O) \Rightarrow C_6H_5O + H \qquad 90\ \%$$

b) formation of phenol by intersystem crossing.

$$C_6H_6 + O(^3P) \Rightarrow (C_6H_6O) \Rightarrow C_6H_5OH \qquad 10\ \%$$

The displaced hydrogen atom reacts efficiently with O_2 to HO_2 at atmospheric pressure [10]

$$H + O_2 + M \Rightarrow HO_2 + M$$

Hydrogen peroxide can be formed from HO_2:

$$HO_2 + HO_2 \Rightarrow H_2O_2 + O_2$$

Hydrogen peroxide photodissociates to hydroxide radicals [3]

$$H_2O_2 + h\nu \Rightarrow 2\ OH$$

The second main reaction product of $O(^3P)$ attack, the phenoxy radical, is able to add molecular oxygen several times with high reaction rates [10,11,12,13]

$$C_6H_5O + O_2 \Rightarrow C_6H_5O_3$$
$$C_6H_5O_3 + O_2 \Rightarrow C_6H_5O_5$$
$$C_6H_5O_5 + HO_2 \Rightarrow C_6H_6O_5 + O_2$$

This peroxy radical probably photodissociates [3] to:

$$C_6H_6O_5 \Rightarrow C_6H_5O_4 + OH$$
$$C_6H_5O_4 \Rightarrow C_4H_4O_2 + C_2HO_2$$

Alkoxy radical fragments and unsaturated aldehydes are created which may add oxygen or photolyze to smaller C/H/O fragments.

The addition of OH (from H_2O_2 photodissociation) to benzene can be assumed to be the first step of a possible further benzene degradation pathway [14,15,16].

Temperatures above 500 K promote hydrogen atom abstraction, while OH-addition occurs even at lower temperatures:

$C_6H_6 + OH \Rightarrow C_6H_7O \qquad T \leq 300K$

$C_6H_6 + OH \Rightarrow C_6H_5 + H_2O \qquad T \geq 500K$

The radical products should easily add molecular oxygen to form peroxy radicals which again photodissociate to give smaller fragments.

Our GC/MS side-product analysis shows that radical attack also leads to substitution of the benzene ring and some build-up of larger aromatic systems, e.g. biphenyl from C_6H_5-radical reactions. Considering the low quantum yields for O_3 senitized photooxidation of benzene and the low yield of benzene substituted products, the OH-channel is probably of minor importance.

The carbonylic C/H/O-fragments formed are probably degraded further via "Norrish fragmentation" after $n \rightarrow \pi^*$ absorption.

type 1: $RCHO + h\nu \Rightarrow R + HCO$ or

$\Rightarrow RH + CO$

type 2: $R_2CHCR_2CR_2CHO + h\nu \Rightarrow R_2CCR_2 + CHR_2CHO$

The formyl radical HCO reacts with molecular oxygen:

$HCO + O_2 \Rightarrow CO + HO_2$ or decomposes to $CO + H$

Oxidation of HCO may finally lead to the HCOOH product we observed.

CO reacts with O-, OH- and HO_2-radicals to CO_2. Mainly H-atom abstraction via OH- and HO_2-attack creates another final product of photooxidation, H_2O.

Up to now, little is known experimentally about intermediate products and their thermal and photolysis rates which would allow a refinement of the reaction mechanism and a reliable kinetic simulation of O_3-sensitized benzene photooxidation.

5. Conclusions

From the results presented here we conclude that photooxidation of exhaust air benzene e.g. from contaminated soil can be made much more efficient by adding ozone externally or using a high-intensity, medium-pressure Hg-

lamp which itself produces sufficient ozone from O_2-photolysis. If the exhaust air is highly charged with chlorinated hydrocarbons, then the ozone produced "in situ" will be destroyed efficiently by the well-known Cl-O_3 cycle. Then it may be favourable to add sufficient ozone externally for degradation of the aromatics in the mixture. The photooxidation of benzene **in the absence of O_3**, however, is inefficient, both at 185 nm and 254 nm.

6. References

[1] Okabe, Photochemistry of small molecules, John Wiley & sons, New York

[2] O.Kajimoto, R.I.Cvetanovic, Int.J.Chem.kinet., 11, 605 (1979)

[3] J.G.Calvert, I.N.Pitts, Jr. Photochemistry, John Wiley & sons, Inc.

[4] A.Yokoyama, X.Zhao, E.J.Hintsa, R.E.Continetti, Y.T.Lee, J.Chem.Phys. 92 (7), 4222 (1990)

[5] S.Sibener, R.J.Buss, P.Casavecchia, T.Hirooka, Y.T.Lee, J.Chem.Phys. 72, 4341 (1980)

[6] R.A.Bonanno, P.Kim, J.H.Lee, R.B.Timons, J.Chem.Phys. 57, 1377 (1972)

[7] N.J.Barry, I.W.Fletcher,J.C.Whitehead, J.Phys.Chem. 90, 4911 (1986)

[8] A.Gonzales Urena, S.M.A.Hoffman, D.J.Smith, R.Grice, J.Chem.Soc.Faraday Trans.2 82, 1537 (1986)

[9] Esser, Dissertation, Universität Heidelberg (1988)

[10] R.Atkinson, Int.J.Chem.Kinet. 12, 779 (1980)

[11] R.Atkinson, W.P.L.Carter, Chem.Rev. 84, 437 (1984)

[12] J.N.Pitts Jr., Int.Chem.Kinet. 11, 45 (1979)

[13] R.Atkinson, Chem. Rev. 86, 69 (1986)

[14] K.Lorenz, R.Zellner, Ber.Bunsenges.Phys.Chem. 87, 629 (1983)

[15] M.Rinke, C.Zetzsch, Ber.Bunsenges.Phys.Chem. 88, 55 (1984)

[16] F.P.Tully, A.R.Ravishankara, R.L.Thompson, J.M.Nicovich, R.C.Shah, N.M.Kreutter, P.H.Wine, J.Phys.Chem. 85, 2262 (1981)

[17] P.Borrel, A.Cervenka, J.W.Turner, J.Chem.Soc.B 12, 2293 (1971)

[18] P.Potzinger, G. von Bünau, Int. Conf. Photochem 1, 242 (1967)

[19] D.S.Herr, W.A.Noyes jr., J.Am.Chem.Soc. 62, 2052 (1940)

[20] P.Potzinger, G. von Bünau, Ber. Bunsenges. Phys. Chem. 72(2), 195 (1968)

[21] K.Foote, M.H.Mallon, J.N.pitts jr., J.Am.Chem.Soc. 88, 3698 (1966)

[22] K.Shindo, S.Lipsky, J.Chem.Phys. 45, 2292 (1966)

[23] H.R.Ward,J.S.Wishnok, P.D.Sherman jr., J.Am.Chem.Soc. 89, 162 (1967)

[24] L.Kaplan, K.E.Wilzbach, J.Am.Chem.Soc. 89, 1030 (1967)

[25] L.Kaplan, S.P.Walch, K.E.Wilzbach, J.Am.Chem.Soc. 90, 5646 (1968)

[26] H.R.Ward, J.S.Wishnok, J.Am.Chem.Soc. 90, 5353 (1968)

[27] F.Mellows, S.Lipsky, J.Phys.Chem. 70, 4076 1966)

[27] N.Nakashima, K.Yoshihara, J.Chem.Phys. 79, 2727 (1983)

[28] N.Nakashima, K.Yoshihara, J.Chem.Phys. 77, 6040 (1982)

[29] J.P.Reilly, K.L.Kompa, J.Chem.Phys. 73, 5468 (1980)

[30] S.A.Lee, J.M.White, W.A.Noyes, J.Chem.Phys. 65, 2805 (1976)

[31] L.Kaplan, K.E.Wilzbach, J.Am.Chem.Soc. 90, 3291 (1968)

[32] A.Passner, S.L.McCall, M.Leventhal, Rev.Sci.Instrum. 47, 1221 (1976)

[33] J.K.Foote, M.H.Mallon, J.N.Pitt jr., J.Am.Chem.Soc. 88/16, 3698 (1966)